RSC Advances

ROYAL SOCIETY OF CHEMISTRY

www.rsc.org/advances

RA-ART-11-2014-015056 R2

Adsorption of sulfamethazine by multi-walled carbon nanotubes: effects of aqueous solution chemistry

Quanquan Yang [a], Guangcai Chen [a,b *], Jianfeng Zhang [a], Helian Li[c]

[a] Research Institute of Subtropical Forestry, Chinese Academy of Forestry, Fuyang, Zhejiang 311400, China

[b] Stockbridge School of Agriculture, University of Massachusetts, Amherst, Massachusetts 01003, United States

[c] School of Resources and Environment, University of Jinan, Jinan 250022, China

[*]Corresponding author.

Phone: 86-571-63105079

Fax: 86-571-63141304

Email: guangcaichen@sohu.com (CHEN GC).

Abstract

The adsorption of sulfamethazine (SMZ) by pristine and hydroxylated multi-walled carbon nanotubes (P-MWCNTs, H-MWCNTs) was studied under varied pH, ionic strength, cations and anions in solution. The results suggest that the SMZ adsorption onto MWCNTs can be depicted well by the pseudo-second-order and Langmuir models. The adsorption of SMZ onto MWCNTs were ionic strength and pH dependent, which indicated hydrophobic and electrostatic interactions, may be the main adsorption mechanisms. The presence of cations at 0.5 mM showed different effects on SMZ adsorption. Cu^{2+} slightly decreased SMZ adsorption by 10% to 20% at solution pH of 2.3 and 4.9, due to the competing effect of Cu^{2+} with SMZ^{+} and $SMZ^{\pm}$. But Cu^{2+} increased SMZ^{-} adsorption by 20% to 60% at solution pH of 7.4 and 10.0, due to the facilitating effect of the complex formation of Cu^{2+}-SMZ. Al^{3+} promoted the SMZ adsorption onto P-MWCNTs, which can be attributed to the facilitating effect of Al^{3+} through metal bridge, while inhibiting the SMZ adsorption by H-MWCNTs, which can be ascribed to the competing effect between Al^{3+} and SMZ for the negative charged functional groups and the shielding effect of adsorbed Al^{3+} with a larger hydrated radius at pH of 2.3, 4.9 and 7.4. SMZ adsorption was slightly decreased with the addition of 0.5 mM anions (Cl^{-}, CO_3^{2-}, SO_4^{2-}, PO_4^{3-}) due to the increase in density of negative charge on the MWCNTs surface. The *μ-FTIR* result showed that π-π interaction may also play an important role in the adsorption process.

Keywords: MWCNTs, sulfamethazine, metal cations, adsorption

1. Introduction

Antibiotics are widely applied all over the world. The fate, distribution, biodegradation and removal of antibiotic residues in the environment have drawn much research interest [1]. Sulfamethazine (SMZ), a major sulfonamide drug [2], is extensively used as a veterinary medicine to control infectious diseases and promote the growth of farm animals. However, most of the SMZ fed to animals cannot be metabolized, up to 90% of SMZ is excreted into the environment via feces and urine [3-5]. SMZ has been frequently detected in surface water [6], groundwater [7], drinking water [8], soil [9] and sediment [10] in agricultural areas, with concentrations ranging from ng·L^{-1} to ug·L^{-1}. Residues of SMZ may impose toxic effects on the soil ecosystem. It has been suggested that SMZ in the soil (53.6 mg·kg^{-1}) has a dramatic short term detrimental effect on readily culturable bacteria, potential metabolic activity, and selected enzyme activities. Moreover, a shift of the microbial populations toward a lower bacterial/fungal ratio was observed after SMZ treatment [11]. In addition, it has been reported that 13 mg·kg^{-1} of SMZ had significant toxic effects on soil respiration and plant growth [12]. Furthermore, SMZ may be accumulated throughout the food chain contribute to acute and/or chronic disease. In sum continued research into the environmental behavior of SMZ is both important and necessary.

Carbon nanotubes (CNTs), first discovered in 1991 [13], have drawn great attention due to their layered and hollow structures, their rich nano porous and high specific surface area [14], and their unique electrical and mechanical properties [15,16]. These

unique structures and properties allow CNTs to have strong interaction with contaminants via non-covalent forces, such as van der Waals forces, electrostatic forces, hydrogen bonding, hydrophobic interactions and π–π interactions [17-19]. Hence, CNTs exhibit excellent adsorption capacity to contaminants, particularly to those containing benzene rings [20,21].

Antibiotics are a type of new emergent contaminant, whose adsorption behavior and mechanism in relation to CNTs have been recently studied [22,23]. Ji et al. (2009) compared the adsorption of tetracycline onto CNTs, activated carbon (AC) and graphite. The results showed the order of adsorption capacities of tetracycline based on unit mass was SWCNT> MWCNT > AC > graphite, while the adsorption affinity of tetracycline decreased in the order of graphite/SWNT > MWNT >> AC after the normalization for adsorbent surface area [22]. Other research suggested sulfamethoxazole adsorption onto CNTs was controlled by hydrophobic intercation and the π-π donor-acceptor system [23].

Antibiotics are usually used together with metal salts as a growth promoter on livestock farms and both may continue to interact in the environment [24]. Previous studies showed cations Cs^{+} and Ca^{2+} may decrease sulfamethoxazole adsorption by CNTs, and the decrease range depended on the concentration of cations in the solution [25]. The suppress effect was also closely related with the solution pH. The addition of Cu^{2+} and Al^{3+} inhibited the adsorption of ionizable sulfathiazole and tylosin contaminants on peat and soil at low solution pH, while Cu^{2+} promoted the adsorption

at high solution pH [26]. The effect of the suppress mechanism was ascribed to the large hydration shell of metal cations which shielded the hydrophobic sites occupied by organic chemicals [27-29]. The presence of anions, such as phosphate, enhanced the adsorption of sulfamethoxazole (SMX) by CNTs in a low pH condition; this increase was ascribed to the formation of ion pairs between phosphate and SMX^+. Increasing the phosphate decreased the electrostatic repulsion between SMX^+ and the positive CNTs' surface [25]. However，there is still a fundamental issue to be understood: what are the underlying solution chemistry characteristics that impact the adsorption of antibiotics by CNTs in aquatic environments?

The current study selected SMZ as the model antibiotic, and the pristine and functionalized multi-walled carbon nanotubes (P-MWCNTs, H-MWCNTs), as the adsorbents. The effects and mechanisms of solution chemistry, including pH, ionic strength, metal cations, and anions on the adsorption of SMZ by the MWCNTs were explored in detail.

2. Materials and methods

2.1. Materials

P-MWCNTs and H-MWCNTs (purity > 95%) with outer diameter of 10 ~ 20nm, surface oxygen contents 0.85% and 7.07%, respectively, were purchased from Chengdu Organic Chemistry Co., Chinese Academy of Sciences. They were synthesized by the chemical vapor deposition method of methane in hydrogen mixture at 700℃ using Ni nanoparticles as the catalyst. The ζ-potential of MWCNTs at

different pH was recorded by a Zeta potential analyzer (Nano-Z, Malvern Instruments, UK.) after the suspension was rotated continuously for 24 hour at 298 K. The detailed structural properties such as specific surface area and pore volume of the MWCNTs were determined and presented in Table S1, which were firstly published in Ref 30.

Sulfamethazine (4-amino-N-[4,6-dimethyl-2-pyrimidinyl] benzenesulfona-mide, in purity > 99%) was purchased from Sigma-Aldrich Trading Co., Ltd (Shanghai, China). The molecular structure and physicochemical properties of SMZ are listed in Table S2. Metal cations ($Al(NO_3)_3$, $Cd(NO_3)_2$, $Cu(NO_3)_2$ and $Pb(NO_3)_2$) and anions (KCl, K_2CO_3, K_2SO_4 and K_3PO_4) were obtained from Sinopharm Chemical Reagent Co., Ltd (Shanghai, China). Ultrapure grade water was used in all experiments. All other chemicals and solvents were of analytical reagent grade or better.

2.2. Batch adsorption

All batch adsorption experiments were performed in 40 mL glass centrifuge vials sealed with Teflon-lined screw-caps. MWCNTs were weighed in the amounts of 8 mg P-MWCNTs or 12 mg H-MWCNTs and 25 mL background solution (0.02 M $NaNO_3$ and 200 mg·L^{-1} NaN_3) containing different concentration of SMZ were filled into vials. The reaction solution was suspended in dark in a constant temperature shaker (HZQ-F160, Huamei Biochemistry Instrument, Soochow, China) with a revolving speed of 150 rpm at 298 K. The solution pH was adjusted by 0.1 M NaOH or 0.1 M HNO_3. The ionic strength was adjusted by $NaNO_3$. Adsorption kinetics and isotherm experiments were run in duplicate and the experiments of effects of aqueous solution

chemistry were run in triplicate.

2.2.1. Adsorption kinetics

Adsorption kinetics of SMZ by MWCNTs was performed at an initial concentration of 20 $mg \cdot L^{-1}$ at pH 5.0 ± 0.1. 36 independent assays vials were conducted and two vials of them were sampled at predetermined time intervals, and a certain amount of the supernatant was filtered through a hydrophilic membrane filter of 0.45 μm after centrifugation at 1000 *g* for 10 min. The sampling time was 10, 20, 30, 40, 60, 90 min and 2, 3, 4, 5, 6, 8, 10, 12, 24, 36, 48, 72 h (the centrifugation time (10 min) was included in sampling time).

2.2.2. Adsorption isotherms

The initial concentration of SMZ was 5, 10, 20, 30, 40, 60, 80 and 100 $mg \cdot L^{-1}$. Solution pH was adjusted to 5.0 ± 0.1. After reaction of 24 h, the MWCNTs and the supernatant were separated as described above.

2.2.3 The effects of aqueous solution chemistry

The initial solution pH ranging from 3.00 to 11.00 was adjusted to explore the effect of pH on SMZ adsorption. During the reaction, the pH was readjusted by adding 0.1 M NaOH or 0.1 M HNO_3 at intervals of 2, 12 and 22h. The effect of ionic strength, varying from 0.02 to 0.2 M $NaNO_3$, was investigated at pH 5.0 ± 0.1. The effect of cations and anions on the adsorption of SMZ onto MWCNTs were investigated at concentration of 0.5 mM metal cations (Na^+ (as a control test), Cu^{2+}, Al^{3+}, Cd^{2+} and Pb^{2+}) or anions (NO_3^- (as a control test), Cl^-, SO_4^{2-} , PO_4^{3-} and CO_3^{2-}) in solution

containing SMZ at concentrations of 10, 20, 40 $mg \cdot L^{-1}$, at solution pH of 2.3, 4.9, 7.4 and 10.0. After the reaction of 24 h, the MWCNTs were separated as described above.

2.3. SMZ determination

In order to eliminate the interference of metal cations coexisted in solution on the quantitative determination of SMZ, the absorbance spectrum of SMZ was scanned with 1800PC ultraviolet-visible spectrophotometer (Shanghai Mapada Instrument CO., Ltd.). The result showed that the presence of metal cations had only slight influence on the maximum absorbance and intensity of SMZ at 263 nm (Fig. S1).

SMZ in the supernatant was determined by High Performance Liquid Chromatography (HPLC, Waters Alliance) equipped with a Waters 478 UV detector at 263 nm and reversed-phase C_{18} column (Waters, 5μm, 3.9mm × 150mm). The mobile phase was methanol and water with volume ratio of 70:30. The injection volume was 30 μL, the flow rate was 1 $mL \cdot min^{-1}$, and the retention time was 1.5 min.

2.4. *μ-FTIR* measurements

The Micro-Fourier transform infrared (*μ-FTIR*) spectroscopic spectrum of adsorbents and adsorbate were measured by a FTIR spectrophotometer (Nicolet 6700, Thermo Nicolet). The samples for *μ-FTIR* analysis were prepared with identical condition to that used in the adsorption experiments. The MWCNTs, MWCNTs-SMZ and MWCNTs-SMZ-Cu were filtered through a hydrophilic membrane filter of 0.45 μm, and washed with ultrapure water and freeze-dried. The samples were placed on a diamond bracket and *μ-FTIR* spectra were measured. The resolution for *μ-FTIR* was

169 8 cm $^{-1}$, and a total 64 scans were collected for each spectrum. The data of spectrum
170 were analyzed with OMNIC software.

171 2.5. Data analysis

172 To account for possible SMZ losses during experiments the recoveries of batch
173 equilibrium experiments were evaluated with vials containing solution without
174 MWCNTs since SMZ losses were smaller than 1%. Therefore, the amount of SMZ
175 adsorbed by MWCNTs was calculated by the decrease of the SMZ concentration in
176 solution using the following equation 1 [31].

177 $$q_e = (c_o - c_e)\frac{V}{m} \qquad (1)$$

178 In the equation, q_e (mg·g^{-1}) is the amount of SMZ adsorbed onto MWCNTs; c_o (mg·L^{-1})
179 and c_e (mg·L^{-1}) are the initial and final concentrations of SMZ, respectively; and V (L)
180 is the solution volume and m (g) is the mass of MWCNTs.

181 Below, the pseudo-first-order model (Eq. 2), pseudo-second-order model (Eq. 3) [32],
182 and intraparticle diffusion model [33] (Eq. 4) were used to fit the adsorption kinetics of
183 SMZ onto MWCNTs.

184 $$\ln(q_e - q_t) = \ln q_e - k_1 t \qquad (2)$$

185 $$\frac{t}{q_t} = \frac{1}{k_2 q_e^2} + \frac{1}{q_e} t \qquad (3)$$

186 $$q_t = k_3 \cdot t^{0.5} + C \qquad (4)$$

187 In all of the above equations, q_e [mg·g^{-1}] and q_t [mg·g^{-1}] are the amount of SMZ
188 adsorbed on MWCNTs at equilibrium and various times t (h). The sorption rate
189 constants are k_1 [h^{-1}], k_2 [g·mg^{-1}·h^{-1}] and k_3 [mg·g^{-1}·h$^{-0.5}$], respectively. In equation 4, C

190 ($mg \cdot g^{-1}$) is the intercept of the vertical axis.

191 The Langmuir [34](Eq.5) and Freundlich [35] (Eq.6) models were employed to fit the
192 equilibrium sorption data of SMZ by MWCNTs.

193 $$q_e = \frac{q_m b c_e}{1 + b c_e} \qquad (5)$$

194 $$q_e = k_F c_e^{1/n} \qquad (6)$$

195 where q_e ($mg \cdot g^{-1}$) is the adsorption at equilibrium; q_m ($mg \cdot g^{-1}$) is the maximum
196 adsorption capacity; c_e ($mg \cdot g^{-1}$) is the equilibrium concentration in solutinon; b
197 ($L \cdot mg^{-1}$) is the affinity parameter; k_F ($mg^{(1-(1/n))} \cdot L^{(1/n)} \cdot g^{-1}$) is the adsorption coefficient;
198 and n is the adsorption constant as an indicator of isotherm nonlinearity.

199 All statistical analysis was performed using Data Processing System (DPS 7.05,
200 Zhejiang University, Hangzhou, China) and plotted with Microcal Origin 7.5
201 (Originlab Corporation, Northampton, MA, USA). A one-way analysis of variance
202 with least significant difference (LSD) test was conducted at a significance level of
203 0.05.

204 **3 Results and discussion**

205 3.1 Adsorption kinetics

206 Adsorption kinetics governs the solute uptake rate and represents the adsorption
207 efficiency of the adsorbents in aquatic solution which varies in solution chemistry
208 characteristics. The C_e/C_0 decreased significantly in the first 2 hours of reaction (Fig.
209 1a), indicated that the SMZ adsorption onto MWCNTs increased significantly in the
210 first 2 hours, which can be ascribed to the large number of vacant sites on the surface

of the MWCNTs. The adsorption rate reduced significantly after 2 hours that followed likewise reinforces the idea that the adsorption became increasingly difficult because of the decrease of vacant surface sites [36]. Still, the adsorption did take place even if at a slower pace. MWCNTs usually exhibit obvious aggregation in aqueous solution and form interstitial and groove sites [37], which are available for SMZ adsorption during this second slow adsorption stage.

Among the three models, the pseudo second-order model, with the highest correlation coefficients (R^2), fits the kinetics data best (Fig. 1b, c, d). Additionally, the comparisons of $q_{e,measured}$ (experimentally measured equilibrium capacity) with $q_{e,calculated}$ (models calculated equilibrium capacity) suggests that the pseudo second-order model is also the best model to fit the adsorption kinetics (Table 1). Thus, the adsorption rate is assumed to be controlled by chemical adsorption [38].

The intraparticle diffusion model assumes the existence of 3 distinct linear regions, which corresponded to the 3 steps on adsorption process, the external surface or instantaneous adsorption, the intraparticle diffusion and the equilibrium plateau, respectively [39,40,41]. It is observed that the adsorption rate was descending in the order of the first step > the second step > the third step (Table 1).

The kinetics results show that the H-MWCNTs had slower and smaller adsorption of SMZ than that of P-MWCNTs (Fig. 1, Table1), despite the former one presenting the larger specific surface area, higher micro and mesopore volumes (Table S1). Hence the surface chemistry such as hydrophobicity and zeta potential of MWCNTs is

most probably playing an important role in the adsorption process, which will be investigated in the following section.

3.2 Adsorption isotherms

The adsorption isotherm of SMZ onto MWCNTs was highly nonlinear, with 1/n values of 0.371 and 0.454 for P-MWCNTs and H-MWCNTs, respectively (Fig. 2, Table 2), which suggests the distribution of adsorption energy of MWCNTs are highly heterogeneous [42]. The Langmuir model fitted the isothermal data better than the Freundlich model with high R^2 values of 0.995 and 0.998 for P-MWCNTs and H-MWCNTs, respectively (Table 2).

The maximum adsorption capacities of P-MWCNTs and H-MWCNTs were approximately 38.13 and 27.29 $mg \cdot g^{-1}$ (Table 2), respectively. The H-MWCNTs had larger specific surface area and pore volume (Table S1), but the adsorption capacity was lower than that of P-MWCNTs, which suggests the functional groups of H-MWCNTs exerted negative effect on the SMZ adsorption. These functional groups decreased the hydrophobicity of MWCNTs in aqueous solution [43]. Consequently, hydrophobic interaction between SMZ and H-MWCNTs is weaker than that between SMZ and P-MWCNTs, making the adsorption of SMZ onto H-MWCHTs less than onto P-MWCNTs. Furthermore, the water molecules around the MWCNTs may be adsorbed on the functional groups and form water dense shell, which may decrease the surface available sites of MWCNT for the SMZ adsorption, and block the access of the SMZ to the active adsorption sites [44], thus decreasing the SMZ adsorption onto

253 H-MWCHTs more than onto P-MWCNTs. In addition, ionized functional groups can
254 adsorb Na^+ from background solution [20], which may increase the diffusion resistance
255 and steric hindrance, thus preventing SMZ from approaching and further interacting
256 with MWCNTs [17,45].

257 3.3. Effect of solution pH

258 The SMZ adsorption by MWCNTs increased slowly with increasing pH from 2 to
259 7, then, decreased abruptly as pH values further increased (Fig. 3a). Tha dsorption of
260 SMZ onto MWCNTs at pH of 7 is about 4 times that of pH at 10.

261 Solution pH has significant effect on both the ionic adsorbate speciation and the
262 surface charge of MWCNTs [43]. SMZ has two pK_a values of 2.28 and 7.42 (Table S2),
263 which can exist as positively charged species (SMZ^+) at pH < pK_{a1} (2.28), negatively
264 charged species (SMZ^-) at pH > pK_{a2} (7.42), and zwitterionic species ($SMZ^{\pm}$) at pH
265 ranging from 2.28 to 7.42 (Fig. S2) [46]. The surface of the MWCNTs was positively
266 charged at pH < pH_{PZC} (4.7 for P-MWCNTs and 1.7 for H-MWCNTs, Fig 3b) and
267 negatively charged at pH > pH_{PZC} [17,47]. Thus, electrostatic interactioe

268 n between the SMZ molecules and the MWCNTs surface is expected to dominate
269 the adsorption process. When pH < pK_{a2} (7.42), the adsorption was enhanced by
270 electrostatic attraction between the opposite charges of the SMZ and the MWCNT
271 surface. The adsorption was suppressed when solution pH > pK_{a2} (7.42) due to the
272 repulsion of the SMZ molecules and the MWCNT surface with the same charges.
273 Furthermore, the hydrophobic partitioning of anionic SMZ at pH > 7.42 is

274 significantly less than in the non-ionized form of SMZ at pH 2.28~7.42 [48]. Therefore,
275 the hydrophobic interactions between MWCNTs and SMZ would decrease when pH
276 increased [46]. Also, the solubility of SMZ increases rapidly as pH increases [49], which
277 helps to account for the decrease in adsorption force between the SMZ and the
278 MWCNTs.

279 3.4. Effect of ionic strength

280 As ionic strength increased from 0.02 to 0.20 M ($NaNO_3$) in solution, the
281 adsorption capacity of SMZ by P-MWCNTs and H-MWCNTs reduced 68% and 87%,
282 respectively (Fig. 4). The increase of ionic strength compresses the electric double
283 layers surrounding MWCNTs which leads to the aggregation of MWCNTs [43,50,51].
284 MWCNTs become more compact and unfavorable for SMZ adsorption due to less
285 available surface adsorption sites [43,51]. The increase of ionic strength also weakens the
286 electrostatic attraction between SMZ^+/$SMZ^\pm$ and MWCNTs because of the decreasing
287 density of negative charge on MWCNTs [51]. Increased ionic strength also enhances
288 competition interaction of the salt ions and the SMZ on surface adsorption sites [43],
289 thus reducing SMZ adsorption.

290 3.5. Effect of metal cations

291 The introduction of metal cations showed different effects on the SMZ adsorption
292 by MWCNTs, which are dependent of solution pH, cations, and carbon nanotubes (Fig.
293 5). The presence of Cu^{2+}, Cd^{2+} and Al^{3+} significantly decreased or increased the SMZ
294 adsorption, while Pb^{2+} showed little influence on the SMZ adsorption by MWCNTs.

295 At three SMZ concentrations, the SMZ adsorption as affected by metal caitons
296 showed insignificant difference, which can be ascribed to the lower molar
297 concentration of of SMZ (40 mg·L^{-1} = 0.144 mM) than that of metal cations (0.5 mM).

298 At solution pH of 2.3 and 4.9, Cu^{2+} slightly decreased the adsorption of SMZ onto
299 P-MWCNTs and H-MWCNTs by 10~20%. This can be attributed to the competition
300 of Cu^{2+} with SMZ^{+} and $SMZ^{\pm}$ for negatively charged adsorption sites on the surface of
301 the MWCNTs [26]. It was reported that the surface complex of Cu^{2+} at hydrophilic
302 defect sites of MWCNTs [28] forms sizable hydration shells of dense water which
303 reduce available sites for SMZ^{+}/$SMZ^{\pm}$ adsorption [52]. The adsorption of Cu^{2+} on
304 MWCNTs may weaken the electrostatic attraction and van der Waals between
305 SMZ^{+}/$SMZ^{\pm}$ and MWCNTs, and may decline the adsorption of SMZ onto MWCNTs
306 at low pH. At pH of 7.4 and 10.0, the dominant SMZ^{-} forms the complexes of
307 Cu^{2+}-SMZ^{-} and Cd^{2+}-SMZ^{-} with a positive charge, which are more easily adsorbed by
308 MWCNTs than SMZ^{-}/$SMZ^{\pm}$ [53]. In addition, Cu^{2+}-SMZ or Cd^{2+}-SMZ are adsorbed on
309 MWCNTs through metal ion bridges [26,54]. Consequently, the presence of Cu^{2+} and
310 Cd^{2+} increased the adsorption of SMZ onto MWCNTs by 20 to 60% at this pH range.

311 For H-MWCNTs, Al^{3+} inhibited the SMZ adsorption at four selected pH values,
312 and reduced the adsorption by 40 to 80% at pH of 10.0. Al^{3+} can compete for the
313 negative charged functional groups of MWCNTs with SMZ. Furthermore, Al^{3+} has a
314 larger hydrated radius [55] which can form dense water shell and significantly block the
315 available sites for SMZ adsorption once Al^{3+} was adsorbed by MWCNTs. Both of

these competing and shielding effects can decrease the SMZ adsorption onto MWCNTs. On the other hand, Al^{3+} can also form the complexes with SMZ, which may facilitate the SMZ adsorption through metal ion bridges. The facilitating or suppressing effects of Al^{3+} on the SMZ adsorption by MWCNTs depend on which force is stronger. The adsorption of metal ions including Al^{3+} by MWCNTs were strongly positively correlated with surface oxygen content [56], suggesting that the H-MWCNTs can adsorb more Al^{3+} than that of P-MWCNTs, indicating the suppressing effect was dominant on the effect of Al^{3+} on the SMZ adsorption by H-MWCNTs. The facilitating effect of Al^{3+} on the SMZ adsorption by P-MWCNTs at pH 2.3, 4.9 and 7.4 can be attributed to the metal bridge of Al^{3+} and SMZ. At pH 10, Al $(OH)_4^-$, the predominant species of Al^{3+}, can interact with SMZ^-, which may increase the electrostatic repulsion between the Al $(OH)_4^-$-SMZ^- and the negative charged surface of MWCNTs, thus decreasing the SMZ adsorption onto both MWCNTs [26]. The specific mechanism of Al^{3+} on the SMZ adsorption needs to be further investigated.

3.6. Effect of anions

The anions such as Cl^-, SO_4^{2-} , PO_4^{3-} and CO_3^{2-} in surface water are usually less than 1 mM [57]. We selected 0.5 mM anion in this experiment to simulate an anion concentration that occurs in real aquatic environments. The results suggest that the presence of anions showed different effects on the SMZ adsorption by MWCNTs. The addition of Cl^- and SO_4^{2-} had little effect on the SMZ adsorption, while the presence of

337 PO_4^{3-} and CO_3^{2-} inhibit the SMZ adsorption by MWCNTs (Fig. 6).

338 When PO_4^{3-} was present in solution, the SMZ adsorption decreased slightly by
339 3.0~13.9% and 2.1~15.1% for P-MWCNTs and H-MWCNTs, respectively. At pH 10,
340 the suppression of the SMZ adsorption reached the maximum by 13.9% and 15.1% for
341 P-MWCNTs and H-MWCNTs, respectively. The suppression effect of PO_4^{3-} on the
342 SMZ adsorption can be attributed to the electrostatic repulsion between anion and the
343 negatively charged surface of the MWCNTs [58]. PO_4^{3-} adsorption may block the
344 available adsorption sites for SMZ through increasing surface negative charge density
345 of the MWCNTs, hence suppressing the adsorption of SMZ by MWCNTs [59]. Another
346 study found the sulfamethoxazole (SMX) adsorption, a similar antibiotic in structure,
347 was enhanced by PO_4^{3-} at pH < 7 [25], however, the current study did not confirm the
348 same effect of PO_4^{3-} on the SMZ adsorption.

349 At pH 10, CO_3^{2-} significantly decreased the SMZ adsorption onto P-MWCNTs by
350 2% to 20% and onto H-MWCNTs by 40% to 55%. The one carbon atom and three
351 oxygen atoms of CO_3^{2-} may form a π-bond. The resulting carbonate adsorbs onto the
352 MWCNTs surface by π-π interaction, reducing the adsorption of SMZ. At pH 2.3, 4.9
353 and 7.4, CO_3^{2-} generates HCO_3^- and H_2CO_3, which weakens π-π interaction. The
354 inhibition effect of CO_3^{2-} on the SMZ adsorption by P-MWCNTs is weaker than that
355 by H–MWCNTs. This is due to H-MWCNTs' oxygen containing functional groups
356 which increase the adsorption density of CO_3^{2-} through enhancing π-π interaction.

357 3.7. *μ-FTIR* analysis

The *μ-FTIR* was performed to explore the adsorption sites of SMZ onto MWCNTs (Fig. 7 and Fig. 8). The important peaks and corresponding vibrations were listed in Table 3. The peaks at 1706/1708 cm^{-1} and 1092/1100 cm^{-1} refer to the C=O and the C-O stretching vibrations, respectively [30], and 1706/1708 cm^{-1} and 1372 cm^{-1} all correspond to the carboxylic group (-COOH) [27,60]. The bands at 1199/1194 cm^{-1} were assigned to the -C=O stretch and to the -OH bonding for the carboxylic groups (-COOH) [61] or symmetric stretching vibration of $-COO^-$ [28].

When SMZ was adsorbed on the MWCNTs, some new peaks appeared at bands 1380~1580 cm^{-1} (Fig. 8). The peak at 1438 cm^{-1} (Fig. 8a) was a C=C stretching vibration of the benzene ring of the SMZ; the peak at 1507/1508 cm^{-1} (Fig. 8a, b) was a scissoring vibration of the NH_2 groups of the SMZ, both indicate the SMZ adsorbed onto the surface of the MWCNTs. At pH of 2.3 and 4.9, the peak at 1717 cm^{-1} (Fig. 8a) was assigned to C=O stretching vibrations of the carboxylic groups (-COOH). As solution pH increased to 7.4 and 10.0, the 1717 cm^{-1} peak disappeared, due to the deprotonation of -COOH at high solution pH [62]. The presence of Cu^{2+} in solution also made the peak at 1717 cm^{-1} (Fig. 8a) declined, indicating that Cu^{2+} was coordinated with the carboxyl group of MWCNTs at low pH [54]. For H-MWCNTs, the benzene ring C=C stretching vibration of SMZ shifted from 1596 cm^{-1} (Fig. 7) [63,64] to 1585 cm^{-1} (Fig. 8b), 1571 cm^{-1}(Fig. 8b), 1571 cm^{-1} (Fig. 8b) and 1588 cm^{-1} (Fig. 8b), respectively, and the benzene ring C-C skeletal vibrations [65] of SMZ shifted from 1385 cm^{-1} (Fig. 7) to 1399 cm^{-1} (Fig. 8b), 1375 cm^{-1} (Fig. 8b), 1380 cm^{-1} (Fig. 8b) and

1382cm^{-1} (Fig. 8b). All of this suggests that the benzene ring of SMZ was partly adsorbed onto the two types of MWCNT by π-π interaction [66,67].

Similarly，for P-MWCNTs, the benzene ring C=C stretching vibrations of SMZ shifted from 1565 cm^{-1} (Fig. 7) [63,64] to 1567 cm^{-1}(Fig. 8a), 1573 cm^{-1}(Fig. 8a), 1558 cm^{-1} (Fig. 8a) and 1562 cm^{-1} (Fig. 8a). The benzene ring C-C skeletal vibrations of SMZ shifted from 1385 cm^{-1} (Fig. 7) to 1382 cm^{-1} (Fig. 8a), 1386 cm^{-1}(Fig. 8a), 1381 cm^{-1} (Fig. 8a) and 1371cm^{-1} (Fig. 8a). The peaks at 1199/1194 cm^{-1} of P/H-MWCNTs (Fig. 7) also shifted to 1201/1189 cm^{-1} (Fig. 8), 1199/1199 cm^{-1} (Fig. 8), 1195/1194 cm^{-1} (Fig. 8) and 1197/1203 cm^{-1} (Fig. 8), which may be ascribed to the interaction of SMZ and P/H-MWCNTs.

4.Conclusion

The results of ionic strength and solution pH on the adsorption suggest that hydrophobic and electrostatic interactions were the major adsorption mechanisms for SMZ onto MWCNTs. The analysis of *μ-FTIR* spectra indicates that the π-π interaction also plays an important role in the adsorption process. The presences of metal cations enhance or inhibit the adsorption of SMZ by MWCNTs, which depended on the type of metal cations, carbon nanotubes and the solution pH value. The selected anions slightly suppressed the SMZ adsorption by MWCNTs at different pH. The results suggest the solution chemistry play an important role in SMZ adsorption by MWCNTs.

Acknowledgment

We sincerely thank Mr. Mark Eugene Reynolds, for English editing of the manuscript. This research was funded by the National Natural Science Foundation of China (21207157), and Shandong Provincial Higher Educational Science and Technology Program (J12LC02). Dr. Guangcai Chen gratefully acknowledges the support from the China Scholarship Council (201303270005).

References

1 S. Managaki, A. Murata, H. Takada, B. C. Tuyen and N. H. Chiem, *Environ sci technol*, 2007, 41, 8004.

2 A.K. Sarmah, M.T. Meyer, A. Boxall, *Chemosphere*, 2006, 65, 725.

3 F. Ingerslev, B. Halling-Sørensen, *Environ Toxicol and Chem*, 2000, 19, 2467.

4 K.-R. Kim, G. Owens, S.-I. Kwon, K.-H. So, D.-B. Lee, Y.S. Ok, *Water, Air, Soil Pollut*, 2011, 214, 163 .

5 L.-J. Zhou, G.-G. Ying, S. Liu, R.-Q. Zhang, H.-J. Lai, Z.-F. Chen, C.-G. Pan, *Sci Total Environ*, 2013, 444, 183.

6 F. Tamtam, F. Mercier, B. Le Bot, J. Eurin, Q. Tuc Dinh, M. Clément, M. Chevreuil, *Sci Total Environ*, 2008, 393, 84.

7 G. Hamscher, H.T. Pawelzick, H. Höper, H. Nau, *Environ Toxicol and Chem*, 2005, 24, 861.

8 A. Watkinson, E. Murby, D. Kolpin, S. Costanzo, *Sci Total Environ*, 2009, 407, 2711.

9 A. Ostermann, J. Siemens, G. Welp, Q. Xue, X. Lin, X. Liu, W. Amelung,

421 *Chemosphere*, 2013, 91, 928.
422 10 X. Liang, B. Chen, X. Nie, Z. Shi, X. Huang, X. Li, *Chemosphere*, 2013, 92, 1410.
423 11 M. Vittoria Pinna, P. Castaldi, P. Deiana, A. Pusino, G. Garau, *Ecotox Environ safe*,
424 2012, 84, 234.
425 12 F. Liu, G.-G. Ying, R. Tao, J.-L. Zhao, J.-F. Yang, L.-F. Zhao, *Environ Pollut*,
426 2009, 157, 1636.
427 13 S. Iijima, *Nature*,1991, 354, 56.
428 14 K. Yang, B. Xing, *Environ Pollut*, 2007, 145, 529.
429 15 T. Ebbesen, H. Lezec, H. Hiura, J. Bennett, H. Ghaemi, T. Thio, *Nature*,1996, 382,
430 54.
431 16 M. Treacy, T. Ebbesen, J. Gibson, *Nature*, 1996, 381, 678.
432 17 B. Pan, B. Xing, *Environ Sci Technol*, 2008, 42, 9005.
433 18 V.K. Gupta, T.A. Saleh, *Environ Sci Pollut Res*, 2013, 20, 2828.
434 19 J.G. Yu, X.H. Zhao, H. Yang, X.H. Chen, Q. Yang, L.Y. Yu, J.H. Jiang, X.Q.
435 Chen, *Sci Total Environ*, 2014, 482-483, 241.
436 20 X. Wang, Y. Liu, S. Tao, B. Xing, *Carbon*, 2010, 48, 3721.
437 21 O.G. Apul, Q. Wang, Y. Zhou, T. Karanfil, *Water Research*, 2013, 47, 1648.
438 22 L. Ji, W. Chen, L. Duan, D. Zhu, *Environ Sci Technol*, 2009, 43, 2322.
439 23 D. Wu, B. Pan, M. Wu, H. Peng, D. Zhang, B. Xing, *Sci Total Environ*, 2012,
440 427-428, 247.
441 24 J Chen, W Chen, D Zhu, *Environ Sci Technol*, 2008, 42, 7225.

442 25 D. Zhang, B. Pan, M. Wu, B. Wang, H. Zhang, H. Peng, D. Wu, P. Ning, *Environ*
443 *Pollut*, 2011, 159, 2616.
444 26Z. Pei, S. Yang, L. Li, C. Li, S. Zhang, X.Q. Shan, B. Wen, B. Guo, *Environ Pollut,*
445 2014, 184, 579.
446 27 G.C. Chen, X.Q. Shan, Y.S. Wang, Z.G. Pei, X.E. Shen, B. Wen, G. Owens,
447 *Environ Sci Technol*, 2008, 42, 8297.
448 28 G.C. Chen, X.Q. Shan, Y.S. Wang, B. Wen, Z.G. Pei, Y.N. Xie, T. Liu, J.J.
449 Pignatello, *Water Res*, 2009 43, 2409.
450 29 G.C. Chen, X.Q. Shan, Z.G. Pei, H. Wang, L.R. Zheng, J. Zhang, Y.N. Xie, *J*
451 *Hazard Mater*, 2011, 188, 156.
452 30 G.C. Chen, X.Q. Shan, Y.Q. Zhou, X.E. Shen, H.L. Huang, S.U. Khan, *J Hazard*
453 *Mater*, 2009, 169, 912.
454 31A.S. Bhatt, P.L. Sakaria, M. Vasudevan, R.R. Pawar, N. Sudheesh, H.C. Bajaj, H.M.
455 Mody, *RSC Adv,* 2012, 2, 8663.
456 32 Y.-S. Ho, *J. Hazard. Mater,* 2006, 136, 681.
457 33 W.J. Weber, J.C. Morris, *J. Sanit. Eng. Div. ASCE,* 1963, 89, 31.
458 34 I. Langmuir, *J. Am. Chem. Soc*, 1918, 40, 1361.
459 35 H.M.F. Freundlich, *J. Phys. Chem*, 1906, 57, 385.
460 36 X. Guo, C. Yang, Z. Dang, Q. Zhang, Y. Li, Q. Meng, *Chem Eng J,* 2013, 223,
461 59-67 (2013).
462 37 F. Wang, J. Yao, H. Chen, Z. Yi, B. Xing, *Environ Pollut,* 2013, 180, 1.

463 38 Y S Ho, G McKay, *Process Biochem*, 1999, 34, 451.

464 39 F C Wu, R L Tseng, R S Juang, *Chem Eng J*, 2009, 153, 1.

465 40 C. Valderrama, X. Gamisans, F.X. de las Heras, J.L. Cortina, A. Farran, *Reactive*

466 *Funct. Polymers,* 2007, 67, 1515.

467 41 A E. Ofomaja, *Bioresour Technol*, 2010, 101, 5868.

468 42 H. Li, D. Zhang, X. Han, B. Xing, *Chemosphere*, 2014, 95, 150.

469 43 X. Ma, S. Uddin, *Nanomaterials*, 2013, 3, 289.

470 44 K. Yang, B. Xing, *Chemical Reviews,* 2010, 110, 5989.

471 45 T. Wang, W. Liu, L. Xiong, N. Xu, J. Ni, *Chem Eng J,* 2013, 215-216, 366.

472 46 S.T. Kurwadkar, C.D. Adams, M.T. Meyer, D.W. Kolpin, *J Agr Food Chem*, 2007,

473 55, 1370.

474 47 Z. Wang, X. Yu, B. Pan, B. Xing, *Environ Sci Technol,*2009, 44, 978.

475 48 W. Lertpaitoonpan, S.K. Ong, T.B. Moorman, *Chemosphere*, 2009, 76, 558.

476 49 Chemical Index Database, Sulfamethazine, CAS Registry Number: 57-68-1

477 http://www.drugfuture.com/chemdata/Sulfamethazine.html .

478 50 D. Lin, N. Liu, K. Yang, L. Zhu, Y. Xu, B. Xing, *Carbon*, 2009, 47, 2875.

479 51 S. Zhang, T. Shao, S.S. Bekaroglu, T. Karanfil, *Water Res*, 2010, 44, 2067.

480 52 J. Chen, D. Zhu, C. Sun, *Environ Sci Technol*, 2007, 41, 2536.

481 53 Y. Sun, Q. Yue, B. Gao, Y. Gao, X. Xu, Q. Li, Y. Wang, *J Taiwan Instf Chem Eng*,

482 2014, 45, 681.

483 54 Z G Pei, X Q Shan, J J Kong, *Environ Sci Technol*, 2009, 44, 915.

55 G. Chen, Y. Wang, Z. Pei, *Environ Sci Pollut Res*, 2014, 21, 2002.

56 F. Yu, Y. Wu, J. Ma, C. Zhang, *J Environ Sci*, 2013, 25, 195.

57 J D Hem, Study and interpretation of the chemical characteristics of Natural Water, *US Geological Survey Water Survey Water Supply Paper*,1985, pp, 2254.

58 T.X. Bui, H. Choi, *Chemosphere*, 2010, 80, 681.

59 Y. Tao, W. Li, B. Xue, J. Zhong, S. Yao, Q. Wu, *J Hazard Mater,* 2013, 261, 21.

60 X.-k. OuYang, R.-N. Jin, L.-P. Yang, Y.-G. Wang, L.-Y. Yang, *RSC Adv,* 2014, 4, 28699.

61 C. Lu, F. Su, *Sep Purif Technol*, 2007, 58, 113.

62 D G Lumsdon, A R Fraser, *Environ Sci Technol*, 2005, 39, 6624.

63 A.M. Mansour, *J Coord Chem*, 2013, 66, 1118.

64 A.M. Mansour, *Inorg Chim Acta*, 2013, 394, 436.

65 V. Udayakumar, S. Periandy, S. Ramalingam, Spectrochim Acta A, 2011, 79, 920.

66 Z. Pei, L. Li, L. Sun, S. Zhang, X.-q. Shan, S. Yang, B. Wen, *Carbon*, 2013, 51, 156.

67 J. Wang, Z. Chen, B. Chen, *Environ Sci Technol,* 2014, 48, 4817.

Figure Legends

Fig. 1 Adsorption kinetics and linear regressions of SMZ by P-MWCNTs and H-MWCNTs (Initial SMZ 20mg·L^{-1}; Temperature: 298K; Initial pH: 5.0 ± 0.1): (a) 0-72hour; (b) pseudo-first-order model; (c) pseudo-second-order model; (d) intraparticle diffusion model.

Fig. 2 Adsorption isotherms of SMZ by P-MWCNTs and H-MWCNTs (Temperature: 298K; Initial pH: 5.0 ± 0.1): The solid line (—) is Langmuir model fiitting; the dotted line (---) is Freundlich model fitting.

Fig. 3 Effect of solution pH on adsorption (a) of SMZ by MWCNTs and the Zeta potential (b) of MWCNTs and.

Fig. 4 Effect of solution ionic strength on adsorption of SMZ by P-MWCNTs and H-MWCNTs (Initial SMZ 20mg·L^{-1}; Temperature: 298K; Initial pH: 5.0 ± 0.1).

Fig. 5 Effect of metal cations on adsorption of SMZ by P-MWCNTs and H-MWCNTs (Temperature: 298K. Different letters (a > b > c > d) means significant differences at a significance level of 0.05.).

Fig. 6 Effect of anions on adsorption of SMZ by P-MWCNTs and H-MWCNTs (Temperature: 298K. Different letters (a > b > c > d) means significant differences at a significance level of 0.05.).

Fig. 7 Micro-Fourier transform infrared spectroscopy spectrum of MWCNTs and SMZ.

Fig. 8 The *μ-FTIR* spectra of adsorbed SMZ and SMZ-Cu complexes on P-MWCNTs (a) and H-MWCNTs (b).

523

524

525

526 **Table 1** The pseudo-first-order model, pseudo-second-order model and intraparticle
527 diffusion model constants of SMZ adsorption by MWCNTs.

1.Pseudo-first-order model					
	$q_{e,measured}$(mg·g^{-1})	$q_{e,calculated}$(mg·g^{-1})	K_1(h^{-1})	R^2	SD
P-MWCNTs	24.38	10.97	0.6590	0.780	0.704
H-MWCNTs	13.32	5.02	0.5514	0.851	0.429
2.Pseudo-second-order model					
	$q_{e,measured}$(mg·g^{-1})	$q_{e,calculated}$(mg·g^{-1})	K_2(g·mg^{-1}·h^{-1})	R^2	SD
P-MWCNTs	24.38	24.78	0.194	0.997	0.005
H-MWCNTs	13.32	13.31	0.486	0.997	0.008
3.Intraparticle diffusion model					
	K_3(mg·g^{-1}·h$^{-0.5}$)			C(mg·g^{-1})	
	1[a]	2[a]	3[a]	1[a]	2[a]	3[a]
P-MWCNTs	20.93	5.54	1.26	3.49	13.33	24.50
H-MWCNTs	10.10	1.67	0.96	3.61	9.31	10.83

528 [a] The 1, 2 and 3 indicated the K_3 or C of 3 distinct linear regions, respectively.
529

Table 2 The Langmuir and Freundlich model fitting adsorption isotherm parameters for adsorption of SMZ by P-MWCNTs and H-MWCNTs.

Carbons	Langmuir			Freundlich		
	q_m(mg·g^{-1})	b(L·mg^{-1})	R^2	k_F (mg$^{(1-(1/n))}$·L$^{(1/n)}$·g^{-1})	n^{-1}	R^2
P-MWCNTs	38.13±0.64	0.072±0.004	0.995	6.73±0.76	0.371±0.030	0.947
H-MWCNTs	27.29±0.38	0.042±0.002	0.998	2.99±0.36	0.454±0.031	0.963

539

540 **Table 3** The important peaks and corresponding vibrations of FTIR spectra of

541 MWCNTs.

Wavenumber (cm^{-1})	bond	Functional group	References
1700-1720	C=O	COOH	62
1596, 1565, 1438	C=C	benzene ring	63, 64
1507,1508	N-H	NH_2	63, 64
1385	C-C	benzene ring	65
1190-1200	-C=O, -OH	COOH	28, 61
1090-1100	C-O	COOH	30

542

543

544

545

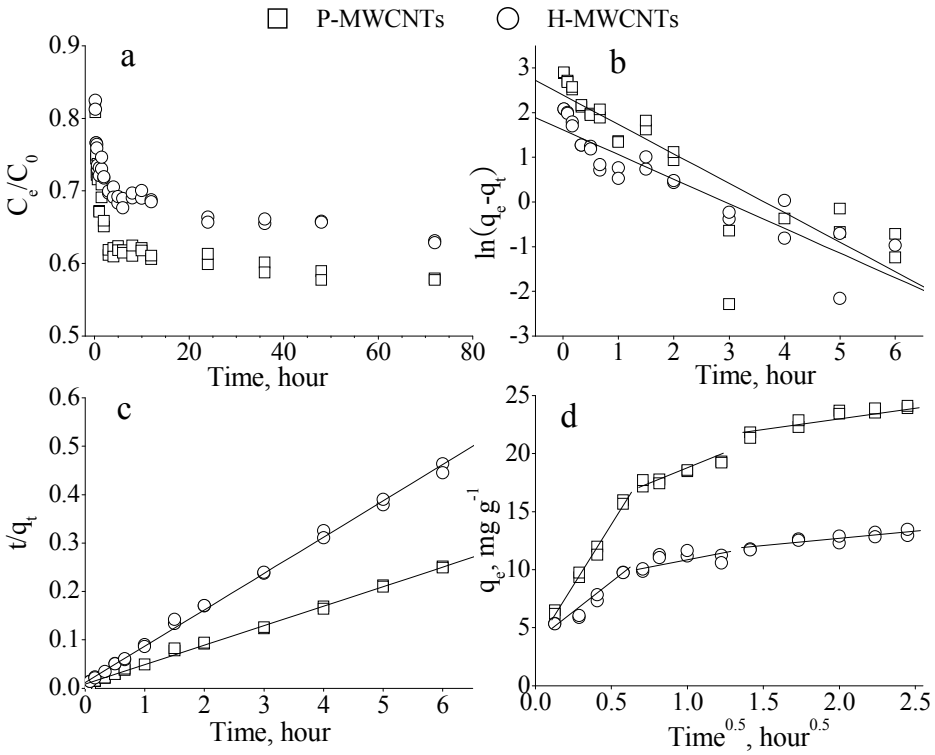

546

547 Fig. 1

548

549

550

551

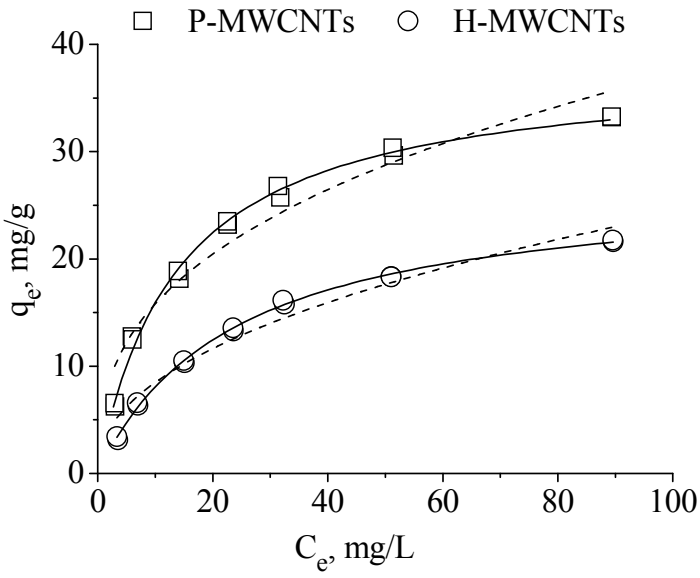

552

553 Fig. 2

554

555

556

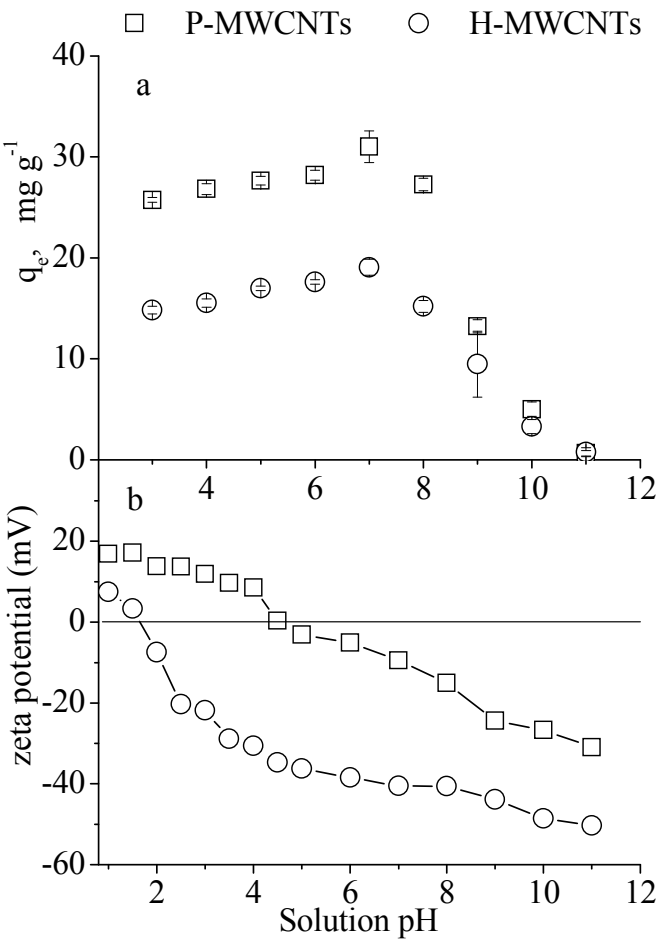

557

558 Fig. 3

559

560

561

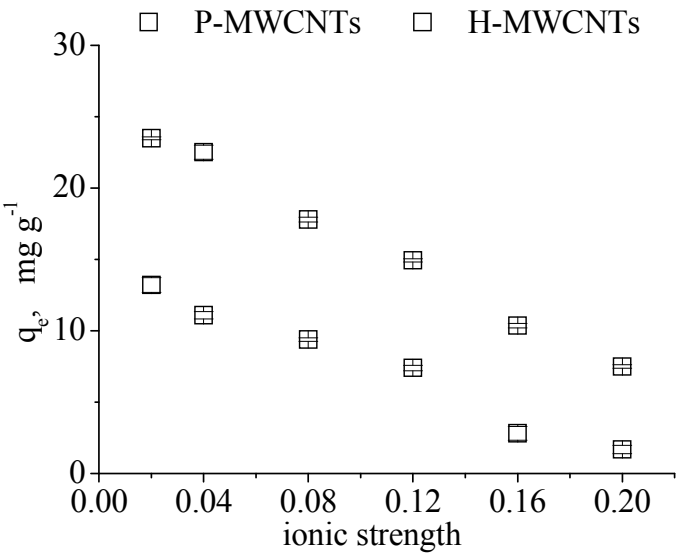

562

563 Fig. 4

564

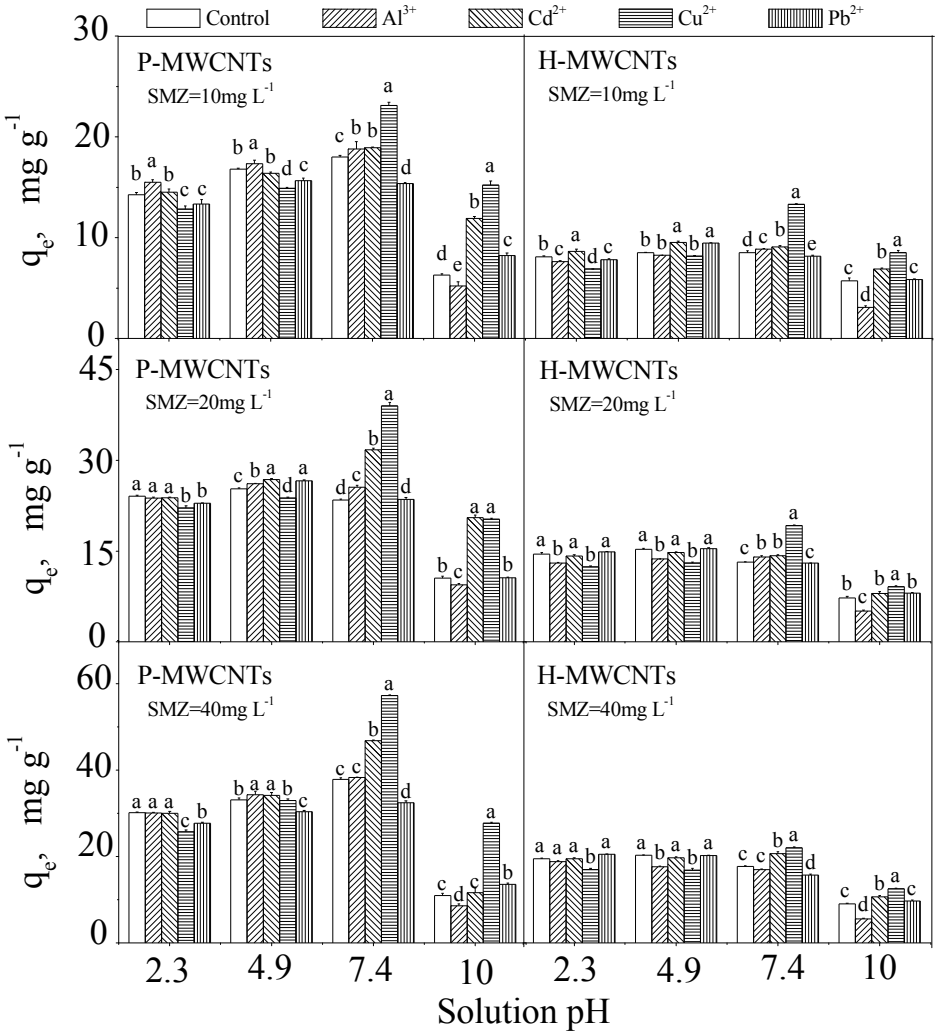

565

566 Fig. 5

567

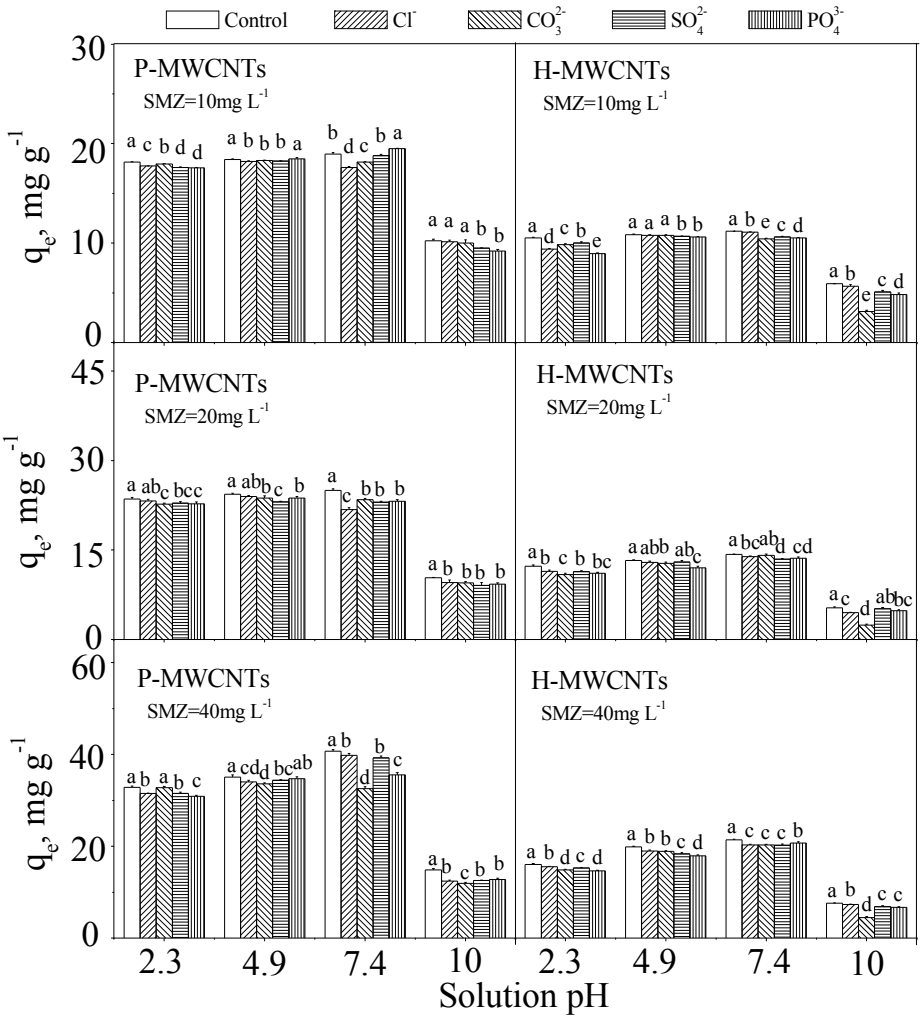

Fig. 6

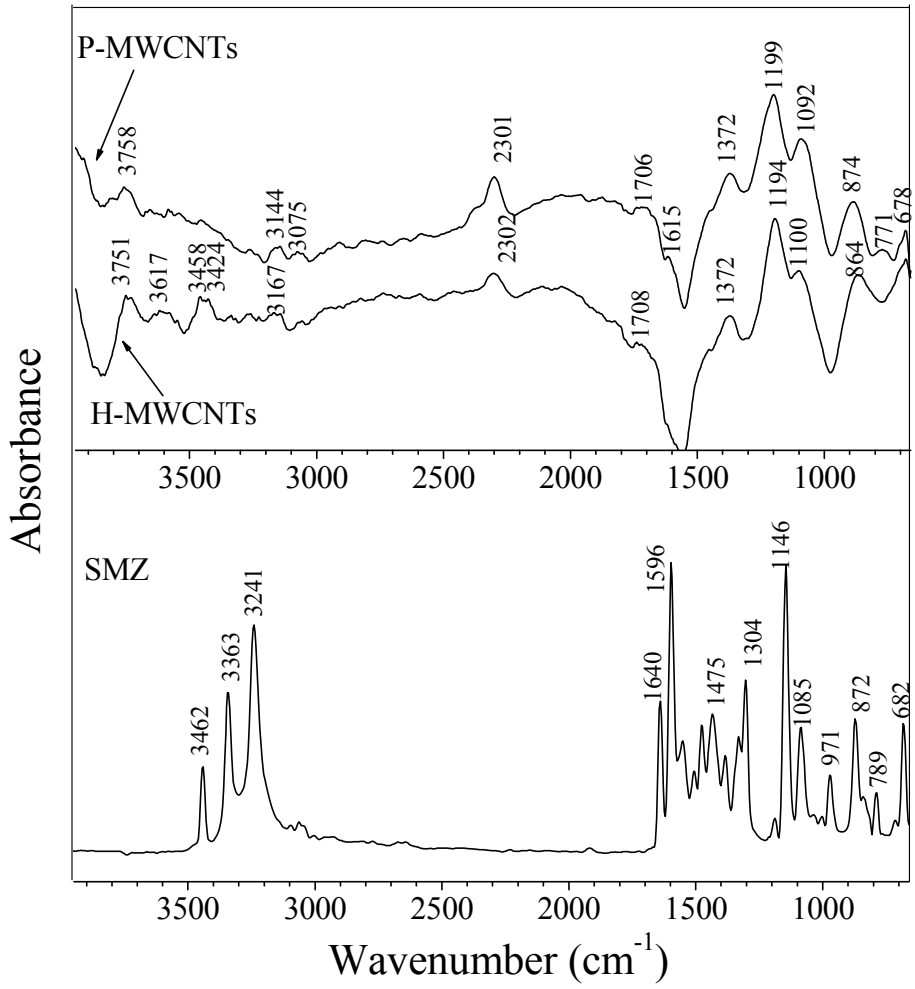

573

574 Fig. 7

575

576

577

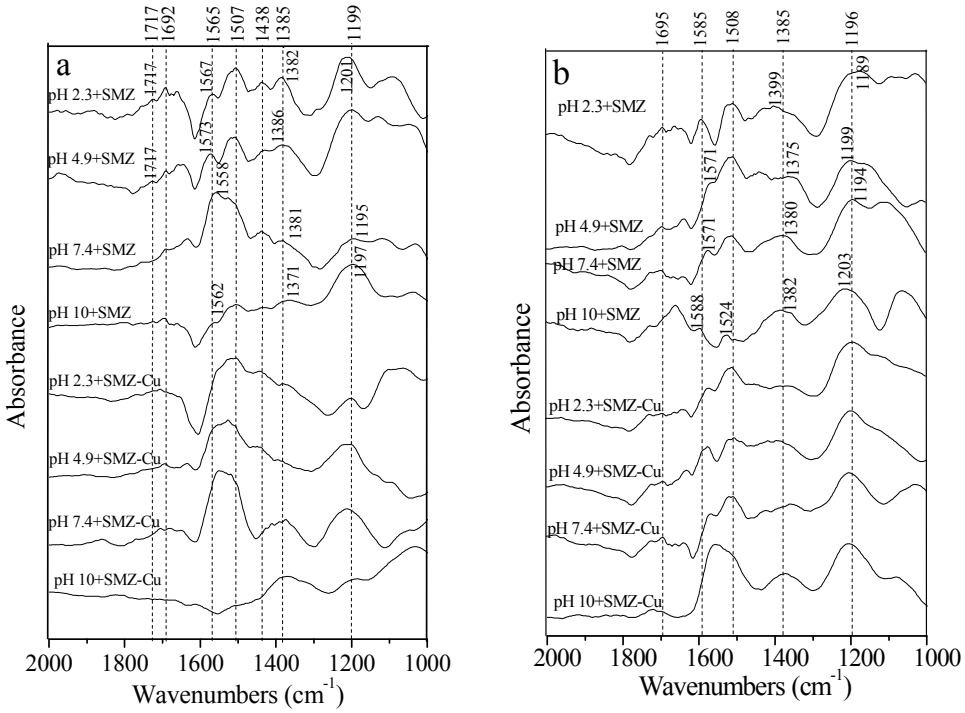

578

579 Fig. 8

580